



# Abbreviations

BSE	Backscattered Electrons
CL	Cliff-Lorimer
EDS	Electron Dispersive X-ray Spectroscopy
EDSX	Electron Dispersive X-ray Spectroscopy
EDX	Electron Dispersive X-ray Spectroscopy
SE	Secondary Electrons
SEM	Scanning Electron Microscope
TEM	Transmission Electron Microscope

# Contents

<b>1</b>	<b>Introduction</b>	<b>2</b>
<b>2</b>	<b>Theory</b>	<b>4</b>
2.1	Theoretical view on characteristic X-rays . . . . .	4
2.1.1	Formation of characteristic X-rays . . . . .	4
2.1.2	Naming convention . . . . .	5
2.1.3	Energy and intensity . . . . .	7
2.2	Empirical view on characteristic X-rays . . . . .	7
2.2.1	From lines to peaks . . . . .	7
2.2.2	Intensity . . . . .	11
2.2.3	K-factors and k-ratios . . . . .	12
2.2.4	Detection system . . . . .	12
2.2.5	Sample thickness . . . . .	12
2.2.6	Bremsstrahlung - the background radiation . . . . .	12
2.3	Calibration of the spectrum . . . . .	12
2.4	SEM . . . . .	13
<b>3</b>	<b>Method / experimental design</b>	<b>14</b>
3.1	Introduction . . . . .	14
3.2	Materials . . . . .	14
3.3	The microscope and the detector . . . . .	14
3.4	Analysis in AZtec . . . . .	15
3.5	Extracting the data . . . . .	15
3.6	Analysis in HyperSpy . . . . .	15
3.7	Data treatment . . . . .	15
3.7.1	Normalization . . . . .	16

3.7.2	Gaussian fitting and peak finding . . . . .	16
3.7.3	Calibration . . . . .	16
3.7.4	Background subtraction . . . . .	16
3.7.5	Area under the peaks . . . . .	17
3.8	Data from Mari? . . . . .	17
<b>4</b>	<b>Results</b>	<b>18</b>
4.1	Introduction . . . . .	18
4.2	Initial quantification . . . . .	18
4.3	Steps in the analysis . . . . .	18
4.4	Calibration . . . . .	18
4.5	Peak and background modelling . . . . .	18
4.6	Background models . . . . .	19
4.7	Failure . . . . .	19
<b>5</b>	<b>Discussion</b>	<b>20</b>
5.1	Introduction . . . . .	20
5.2	Calibration . . . . .	20

# Chapter I

## Introduction

The main goal of this project is to improve EDS analysis. There are multiple ways to do this. One way is to make the analysis more transparent, which would make it easier to understand and use. A second option is to improve the input parameters of the analysis by control checking the instrument with a known sample. A third way is to make the quantitative analysis more accurate, which would improve EDS analysis. In this project, the main focus have been trying to improve the transparency of the analysis. Thus, the problem statement was formulated as:

**How can the transparency of the steps in the EDS analysis be improved, so that the analysis is easier to understand and use?**

With this problem statement, the following sub-problems were formulated:

- How accurate are the out-of-the-box quantification in AZtec and HyperSpy?
- What are done with the data at the different steps in the analysis?
- How is the spectrum calibrated, and is AZtec different than HyperSpy?
- How can the peaks and the background be modelled in a way that is easy to understand?
- How does different background models affect the quantitative analysis done in HyperSpy?
- When does the analysis fail, both in AZtec and HyperSpy?

**(Question for Ton: Should I have a short paragraph here about the status of EDS analysis today?)**

One of the main problems with the existing software for EDS analysis is that they are like black boxes. The manufacturer of EDS sensors, like EDAX, Hitachi, Thermo Fisher Scientific, and Oxford Instruments **(Question for Ton: Cite this?)**, provide their own software for analyzing EDS data. These software packages are black boxes, because the code is hidden, and the users does not know what is happening inside the software. In other words, the user pushes

some buttons to start the analysis of their sample, and then the software does some "magic" to analyze the data and produce some results. The user has few options to change the analysis to fit their needs. Many users tend to accept the results **(Question for Ton: Need to cite something here?)** from the software without questioning them, even though the analyzation "magic" differs between software packages and might be unreliable. The manufacturer Hitachi have trouble with separating Cs from ??, and their solution is to neglect the existence of Cs **(Brynjar: Find citation)**. The manufacturer Oxford Instruments provides the software AZtec which have trouble with ??, and their solution is ?? **(Brynjar: Find something, eg. zero peak)**. Even if the software is not wrong, the user might not understand the results, and the user have no way to change the analysis to fit their needs. Some might say that using e.g. AZtec is EDS analysis for dummies. One could solve this problem with an increase in transparency, because that would make it easier to understand EDS analysis and easier for users to adapt the analysis to their own needs.

**(Brynjar: Dispersion, offset, energy resolution?)**

**(Brynjar: Other parameters of EDS analysis?)**

**(Brynjar: Improving quantitative EDS analysis?)**

## Chapter 2

# Theory

Energy dispersive X-ray spectroscopy (EDS) is a technique for analyzing the elemental composition of a sample with a spatial resolution, used in SEM and TEM. The technique is based on excitation of core shell electrons, which are bound to the atom with different strengths in different elements, and thus the electron relaxation results in very specific photon energies. EDS can be used to determine both the qualitative and quantitative composition of a sample. This chapter will cover the theoretical formation of characteristic X-rays, the empirical adjustments done due to creation and detection issues, explain quantitative calculations, cover the parameters of a quality control program, and briefly explain the basics of a SEM.

### 2.1 Theoretical view on characteristic X-rays

This section is primarily based on Hollas [2, Ch. 8.2] and Goldstein [1, Ch. 4.2]. It covers the theoretical physics behind creation of characteristic X-rays.

#### 2.1.1 Formation of characteristic X-rays

The formation of characteristic X-rays is an inelastic quantum mechanical scattering process in two steps. In the following four equations the subscripts are referring to specific electrons in order to distinguish between them, which is also used in FIGURE XX (Brynjar: make this figure). In the first step described in Equation (2.1) electron  $e_1^-$  from the incident electron beam eject electron  $e_2^-$  from the core orbital of atom A [2, Eq. (8.12)].

$$e_{1\text{incident}}^- + A \rightarrow e_{1\text{outgoing}}^- + A^+ + e_{2\text{ejected}}^- \quad (2.1)$$

The incident electron from the beam loose energy to both breaking the binding energy of the core orbital and to the kinetic energy of the ejected electron. The energy is given by Equation (2.2). The user can control the incident electron energy  $E_{1\text{incident}}$  by the acceleration voltage  $V_{\text{acc}}$  of the electron gun (and the current  $I_{\text{beam}}$  of the electron beam). The

energy of the characteristic X-ray is dependent on the binding energy of the core orbital,  $E_{2\text{-core shell, binding}}$ . In EDS  $E_{1\text{outgoing}}$  and  $E_{2\text{kinetic}}$  serve no purpose [1, Eq. (4.1)].

$$E_{1\text{incident}} = E_{1\text{outgoing}} + E_{2\text{core shell, binding}} + E_{2\text{kinetic}} \quad (2.2)$$

In the second step electron  $e_3^-$  from a higher energy orbital relaxes to the hole in the core orbital of atom A, and the difference in energy is emitted as a photon with a specific energy  $h\nu$  called the characteristic X-ray [2, Eq. (8.12)].

$$e_{3\text{outer shell}}^- \rightarrow e_{3\text{inner shell}}^- + h\nu_{\text{X-ray}} \quad (2.3)$$

The energy of the characteristic X-ray is the difference in energy between the ionized orbital and the orbital filling the hole, shown in Equation (2.4). The equation specifies the energy of the X-ray as  $h\nu$ , but Section 2.2 explains why users of EDS just use the energy directly, usually measured in eV or keV [1, Eq. (4.2b)].

$$h\nu_{\text{X-ray}} = E_{2\text{core shell, binding}} - E_{3\text{outer shell, binding}} \quad (2.4)$$

In the second step in Equation (2.3) it is also a probability that the relaxation energy is used to eject and give kinetic energy to another electron from a higher energy orbital. This process results in two ejected electrons, both the ionized electron from the core orbital and a second ejected electron from a higher energy orbital. The second ejected electron is called an Auger electron. Auger electrons are used for surface studies, because they can penetrate around 2 nm solid material and thus does not escape from inside the sample. The X-rays are emitted in all directions and penetrate typically 4000 nm, and are the signal in EDS. The ratio between the characteristic X-ray photons and Auger electrons are known as the fluorescent (quantum) yield,  $\omega$ .

$$\omega = \frac{\text{X-ray photons}}{\text{Auger electrons}} \quad (2.5)$$

The fluorescent yield is heavily dependent on the experimental setup and can be approximated, which is covered as one of the empirical factors in Section 2.2.

### 2.1.2 Naming convention

The transition lines are grouped and named semi-systematic, based on the orbital the vacancy is in, and the orbital the electron is relaxed from. The naming convention is semi-systematic because it is the original empirical system published in Nature by the Swedish physicist Siegbahn in 1916 [3], when they did not have the knowledge we have today. The International Union of Pure and Applied Chemistry made a more systematic naming convention for X-ray lines which is supposed to be the official one [1, Ch. 4.2.4]. However, the Siegbahn notation is used in the X-ray booklet, in HyperSpy, and by the TEM group at NTNU, and thus is used in this thesis.



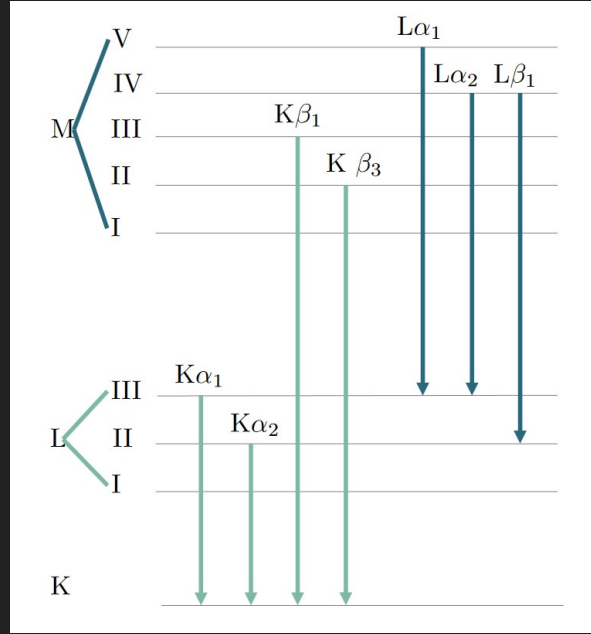


**Figure 2.1:** Direct copy of Maris Figure 2.9. I will make my own.

The X-rays are first named by which shell in the Bohr model the vacancy is in, i.e. the principal quantum number  $n$  of the vacancy orbital. Relaxations to the innermost shell  $n = 1$  is named K-transitions, relaxations to  $n = 2$  is L-transitions, relaxations to  $n = 3$  is M-transitions.

The X-rays are further grouped with Greek letters in families. Orbitals close in energy are usually in the same group, which means that electrons in the same shell usually are in the same family. This naming is non-systematic, but tends to follow a pattern where the transitions labeled  $\alpha$  are the lower energy transitions corresponding to the  $n + 1$  orbitals, and the transitions labeled  $\beta$  are the higher energy transitions corresponding to the  $n + 2$  orbitals. For example,  $L \rightarrow K$  are  $\alpha$ -transitions.

In addition, the lines in an X-ray group are labeled with subscript numbers which generally start with the highest intensity. This is a splitting of the lines due to different energy levels of the orbitals in the same shell. The different energy levels are due to the spin-orbit coupling, which is the interaction between the electron spin and the orbital angular momentum. The spin-orbit coupling increase with increased  $Z$ , which separates the lines more and more. The splitting of the  $\alpha$  family to  $\alpha_1$  and  $\alpha_2$  are usually first resolvable in EDS for elements heavier than tin with  $Z = 50$  [2, Ch. 8.2.2.3].

Putting these three naming conventions together, we name the transition  $L_3 \rightarrow K_1$  as  $K\alpha_1$ , and  $L_2 \rightarrow K_1$  as  $K\alpha_2$ , with more examples in Figure 2.1. The transition  $L_1 \rightarrow K_1$  has  $\Delta l = 0$  and is thus forbidden by the selection rules, see Equation (2.6). In gallium the  $K\alpha_1 = 9251.74$  eV and  $K\alpha_2 = 9224.82$  eV [4] are coupled, but as shown in Figure 2.5 this energy difference of  $\Delta E = 26.92$  eV is too low to be resolved in EDS.

### 2.1.3 Energy and intensity

The energy of the characteristic X-ray depends on which orbital the vacancy is in, which orbital the electron is relaxed from, and the amount of protons in the core of atom A. Higher Z means higher energy of the characteristic X-ray line, because the energy difference between the relaxation orbital and the ionized orbital is larger. Atoms with higher Z have more possible transitions, because they have more electrons and orbitals.

The selection rules, which govern the allowed transitions for the formation of characteristic X-rays, are based on the Pauli exclusion principle and the spin-orbit coupling. See Figure 2.2 for illustration of the quantum number  $n$  and  $l$  which are relevant for the selection rules, while the quantum number  $l$  is dependent on the non-geometrically dependent spin and  $l$ . The selection rules in Equation (2.6) is for the electron which relaxes to the vacancy in the core orbital of atom A [2, Sec. 8.2.2.2].

$$\Delta n \geq 1; \quad \Delta l = \pm 1; \quad \Delta j = 0, \pm 1 \quad (2.6)$$

Even though heavy atoms like gold have more than 30 possible transitions, only a few are detectable in EDS. Lines which are undetectable have low abundance, are too close to other lines, or are forbidden by the selection rules [1, Ch. 4.2.3]. Lines which are detectable have an intensity dependent on the amount of the element in the sample, because a higher amount gives more counts in the detector. The counts in EDS the number of X-ray photons detected in a specific energy range. The energy range is typically around 10 eV. In theory, the ratio of the atomic concentration between two elements are proportional to the ratio of the corresponding lines from the elements. However, there are many factors which affect the intensity of the lines, which are covered in Section 2.2.

## 2.2 Empirical view on characteristic X-rays

On top of the theoretical physics there are many experimental processes affecting both the creation and the detection of characteristic X-rays. The scientific community uses an empirically influenced approach in EDS analysis. This approach includes empirical equations to deal with the imperfect beam, scattering in the chamber, secondary scattering (?), imperfect detectors, ...

**(Question for Ton: What do I do with the thin film assumptions? How do I mention it?)**

### 2.2.1 From lines to peaks

A striking difference between the theoretical and the empirical view is that the lines are not lines, but peaks with a varying width. This is illustrated both in Figure 2.4 and in Figure 2.5, where we see that the two  $K_{\alpha}$  lines of Ga is merged into one broad peak. The peaks in the EDS spectrums have a Gaussian shape, which is a result of the broadening of the lines. The broadening of the lines is due to ... **(Question for Ton: What is the cause of the broadening? And why is it Gaussian?)**. Figure 2.3 shows that lower energy lines are narrower than higher energy lines. This increase in

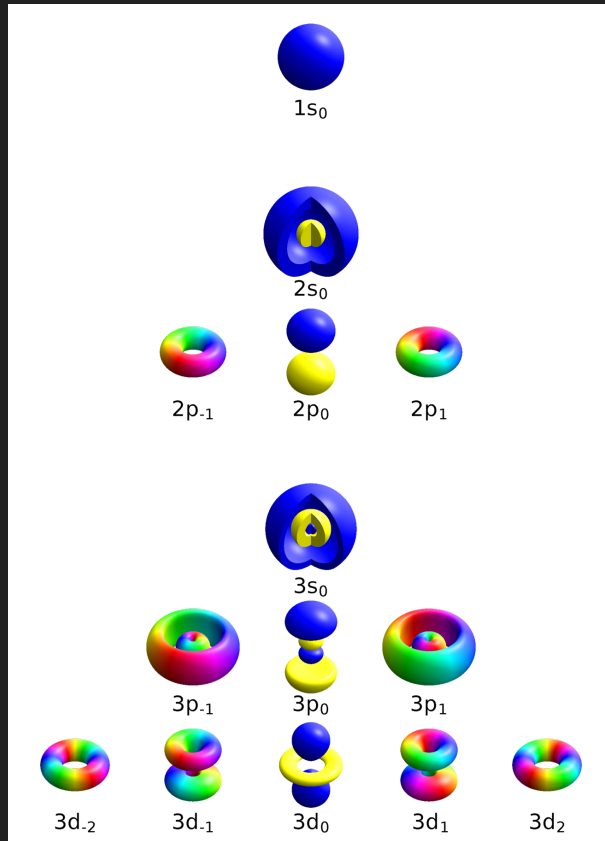


**Figure 2.2:** The quantum numbers  $n$ ,  $l$ , and  $m$  in a hydrogen-like atom. The principal quantum number is shown as the block with values  $n = 1, 2, 3$ . The Azimuthal quantum number is the rows as  $l = s, p, d$ . The magnetic quantum number is the columns as  $m = -2, -1, 0, 1, 2$ . The spin quantum number,  $s$ , is not geometrically dependent and thus not shown. The total angular momentum quantum,  $l$  number is the sum of  $l$  and  $s$ . The figure is copied from the article "Quantum number" on Wikipedia, made by Geek3 - Own work, Created with hydrogen 1.1, CC BY-SA 4.0, <https://commons.wikimedia.org/w/index.php?curid=67681892>.

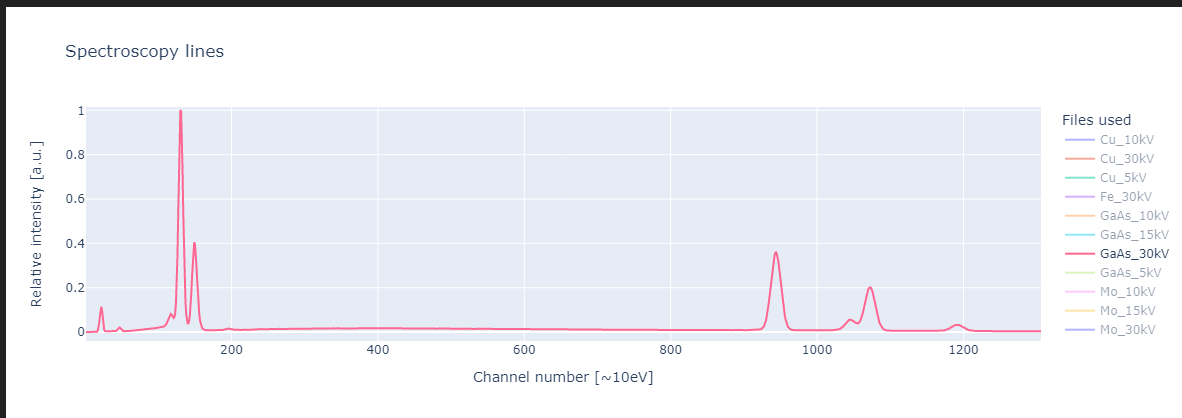


**Figure 2.3:** The whole GaAs spectrum. The next two figures zoom in on different parts of this plot. Data from the SEM Apreo at NTNU NanoLab, 30 kV.

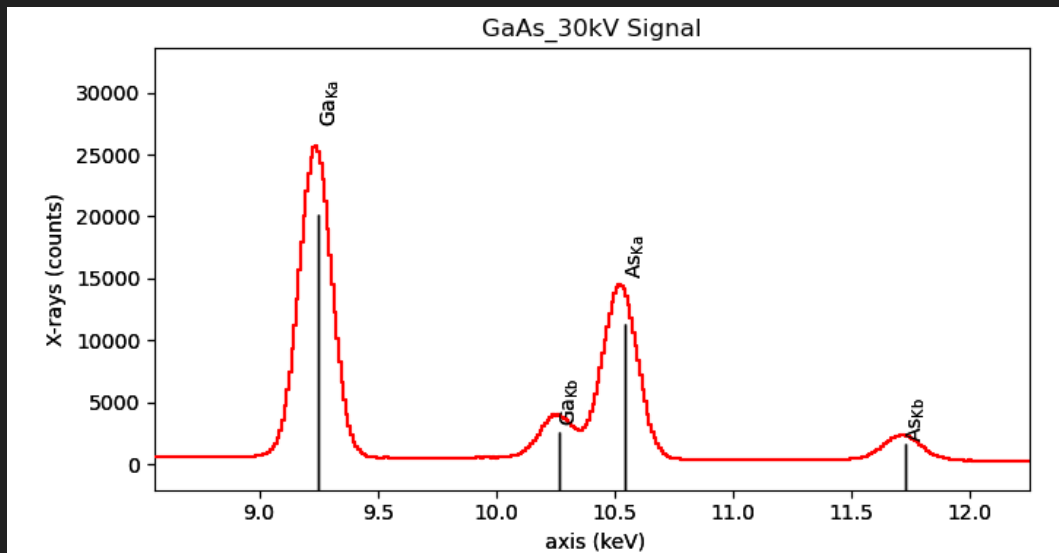


**Figure 2.4:** Plot produced by HyperSpy of the X-ray lines in GaAs from 8 to 12.5 keV. The theoretical lines are marked with black lines, but in reality the lines become peaks with Gaussian shapes. The height of the black lines are empirically estimated and are available in HyperSpy. Notice also how the center of the peak and the black line are slightly right shifted, which can be solved by calibrating the energy scale, see Section 2.3. Data from the SEM Apreo at NTNU NanoLab, 30kV.

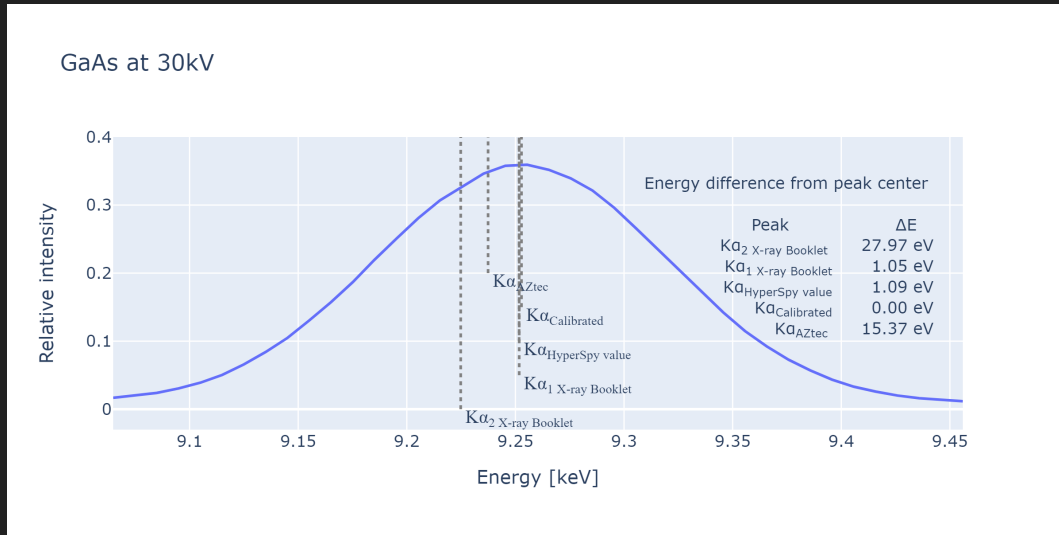


**Figure 2.5:** The theoretical lines  $K\alpha_1 = 9.25174$  and  $K\alpha_2 = 9.22482$  from the X-ray booklet with  $K\alpha = 9.251$  from HyperSpy and the fitted peak  $K\alpha$ . The spectrum is calibrated to Ga  $L\alpha$  and As  $K\alpha$ , where the energy of the peaks is taken from HyperSpy. HyperSpy gives Ga  $K\alpha$  almost directly on top of the theoretical  $K\alpha_1$ . This figure show that the lines which are separated with small energy differences are so close that they make one single peak in the EDS spectrum. Data from the SEM Apreo at NTNU NanoLab, 30kV. **(Question for Ton: This is more results than theory I would say. But I do remember you saying something about having this in the theory section.)**

**Table 2.1:** Ga lines from HyperSpy cite ?? and X-ray booklet [4]. \*\* HyperSpy operates with a single line for each  $K$  and  $L$  shell, but the X-ray booklet lists two lines for each shell. \* HyperSpy lists  $Ln$ ,  $Ll$  and  $Lb_3$  as separate lines, but I am not sure what they correspond to in the X-ray booklet. TODO: Figure out this, eventually just dropping the additional lines.

	X-ray booklet	HyperSpy	HyperSpy
	Energy [keV]	Energy [keV]	Weight, unitless
$K\alpha_1$	9.25174	9.2517	1.0
$K\alpha_2$ **	9.22482		
$K\beta_1$	10.2642	10.2642	0.1287
$L\alpha_1$	1.09792	1.098	1.0
$L\alpha_2$ **	1.09792		
$L\beta_1$	1.1248	1.1249	0.16704
$Ln$ *		0.9843	0.02509
$Ll$ *		0.0544	0.9573
$Lb_3$ *		0.0461	1.1948

broadening with higher energy is due to ... **(Question for Ton: What is the cause of the broadening with higher E again?)**

### 2.2.2 Intensity

The intensity, or weight, of a line is dependent on multiple empirical and physical factors. This subsection will briefly cover fluorescent yield, critical ionization energy, and empirical weights in HyperSpy. In practice, the weight of the lines are included as a part of the k-factors or k-ratios, which are presented in Section 2.2.3. Only the strongest lines are listed in the X-ray booklet, where the theoretical values of the characteristic X-ray lines are listed. The list include:  $K\alpha_1$ ,  $K\alpha_2$ ,  $K\beta_2$ ,  $L\alpha_1$ ,  $L\alpha_2$ ,  $L\beta_1$ ,  $L\beta_2$ ,  $L\gamma_1$ ,  $M\alpha_1$  [4].

**(Brynjar: This info about fluorescent yield is interesting, but will I actually use it?)** The fluorescent yield  $\omega$  is non-linearly dependent on  $Z$ . Figure (4.3) in Goldstein [1] **(Question for Ton: Reproduce the figure? Would take like 2h to use the Crawford data properly I guess)** shows the fluorescent yield for the first 90 elements (which is based on Crawford 2011). For K- and L-shell fluorescent yield,  $\omega$  is strictly increasing. For M-shell fluorescent yield,  $\omega$  is strictly increasing till around  $Z = 80$ , and then it starts to decrease. The figure also show that for the same element  $\omega_K > \omega_L > \omega_M$  **(Brynjar: But L-peaks are higher in the spectra. Explain this in the discussion?)**. When dealing with thin samples, the fluorescent yield can be approximated by an empirical formula based on tin. The formula is given in Equation (2.7), where  $a = 10^6$  for K-shell. **(Brynjar: What is it for L and M? Also, is it really relevant here?)** The two key takeaways from this formula is that  $\omega$  is dependent on  $Z$ , but kinda similar for close elements like Ga  $Z = 31$  and As  $Z = 33$ .

**(Brynjar: Find the source for this formula. Ton said it is from Williams and Carter. Is it valid for bulk? The K-shell have the same shape as Figure 4.3 in Goldstein.)**

**(Question for Ton: I'm not sure if I will actually use this formula, should I just remove it? And I don't get how this formula just becomes a part of the k-factor. Except from the key takeaways mention above.)**

$$\omega = \frac{Z^4}{a + Z^4} \quad (2.7)$$

The critical ionization energy,  $E_C$ , is the energy the incident beam need to ionize a core electron in an atom. If the energy of the incident beam is lower than  $E_C$ , the core electron is not ionized and no peak can be detected. The critical ionization energy is dependent on the atomic number,  $Z$ , of the atom. Higher  $Z$  means higher  $E_C$ , because the core electrons are bound stronger to the nucleus. When the incident beam has an energy higher than  $E_C$  and continues to increase, the amount of ionization is not constant and not linear. The amount of ionization with varying energy above  $E_C$  is dependent on the ionization cross section and the overvoltage, which again are dependent on what shell the ionization happens in. The solution to this is empirically estimations and using k-factors where all factors like this is either cancelled out or included in the k-factor correction.

**(Question for Ton: Is this good enough? If not, what do I write about the ionization cross section and**

overvoltage? What Mari wrote is for thin samples, I think. Why include it if I'm not going to use any equations about the ionization cross section or overvoltage? You said something about just write that intensity it is lower for low energy because of many reasons (absorption, efficiency), with the same reason that background is lower for low energy. But I kinda need to explain some of the reasons to use them in the discussion. Another question: in the k-factor all these other factors fall out, so EDS-people does not use these equations. Am I wrong?)

HyperSpy have an integrated list of the characteristic X-rays, with both the energy and the weight of the lines. (Brynjar: I guess the weights are empirically estimated, but I have not found any information about how they are estimated. In addition: I'm not sure if HyperSpy adjust the line height to the spectrum, or if it knows that Ga Ka are higher than As Ka as in Figure 2.4.) Goldstein uses different intensity weights for isolated atoms, thin foils and bulk samples [1, Ch. 4.2.6], and all are dependent on the atomic number and ionized shell. One could venture down the rabbit hole of finding the theoretical weights for different lines, but that will not be done in this thesis. Examples of the weights from HyperSpy are given in Table 2.1. (Question for Ton: OK?)

### 2.2.3 K-factors and k-ratios

About em k-factors and k-ratios.

### 2.2.4 Detection system

Detector efficiency, detector resolution, dead time, angle/placement of detector, beam issues, stray: secondary excitations in the sample, Si stray, holder / chamber stray detection.

### 2.2.5 Sample thickness

Thin vs bulk samples.

### 2.2.6 Bremsstrahlung - the background radiation

Why linear and why sixth order polynomial. Which are better. (Brynjar: I might use background removal as some results, but I'm not sure. That would be comparing the different methods, and looking at smoothing of the data before removing the background.)

## 2.3 Calibration of the spectrum

$E_1$  and  $E_2$  is the energy of the two characteristic X-rays, and  $c_1$  and  $c_2$  is the channel number of the two characteristic X-rays.

$$\text{Dispersion} = \frac{E_2 - E_1}{C_2 - C_1} \quad (2.8)$$

Get as little extrapolation as possible by selecting the longest possible distance between the two characteristic X-rays, while still using peaks with good signal to noise ratio. **(Brynjar: Quantify signal to noise ratio?)** Assume calibration on one spectrum and use it on all spectra for the same instrument.

Zero-offset in channels is:

$$\text{Zero-offset in channels} = C_1 - E_1 \cdot \text{Dispersion} \quad (2.9)$$

## 2.4 SEM

- how (e-beam, vacuum, ...) - hardware (scanning coils, astigmatism) - imaging (contrast, SE, BSE)



## Chapter 3

# Method / experimental design

### 3.1 Introduction

The data I needed ...

Thanks to Mari (ref) and Martin (ref) who made manuals for easily extracting data from AZtec. The relevant material for data extraction is available on the GitHub repository for this project (ref)

### 3.2 Materials

EDS data was collected on one sample with different sections containing different materials. A half 2" Si wafer was mounted with Cu tape on an Al FIB stub. On the Si wafer a smaller piece of a GaAs wafer was mounted with Cu tape. A Mo disk was mounted to the Si wafer with Ag paint. In the middle of the Mo disk there was a hole where a TEM grid was mounted. The TEM grid had GaAs nanowires on it, and the grid was made of Mo with C film.

### 3.3 The microscope and the detector

The data in this project was collected with the SEM Apreo from FEI with an Oxford EDX detector at NTNU NanoLab. The detector is an EDX Oxford Xmax 80 mm<sup>2</sup> Solid angle detector, with reported energy resolution of 127 eV (Cite: [ntnu.norfab.no](http://ntnu.norfab.no) on the instrument). The acceleration voltage,  $V_{acc}$ , can be set from 0.2 to 30 kV. The beam current,  $I_{beam}$ , has a maximum value of 400 nA. The SEM has an adjustable working distance. The SEM is equipped with a BSE and a SE detector.

The data collection was done on 5, 10, 15, and 30 kV. The beam current was 0.2, 0.4, 0.8, or 1.6 nA, depending on the dead time of the detector, trying to get the dead time around 30%. All samples were collected on 2048 channels ranging from 0 to 20 keV. Working distance was 10 mm. Processing time was set to 5 and each spectrum was collected

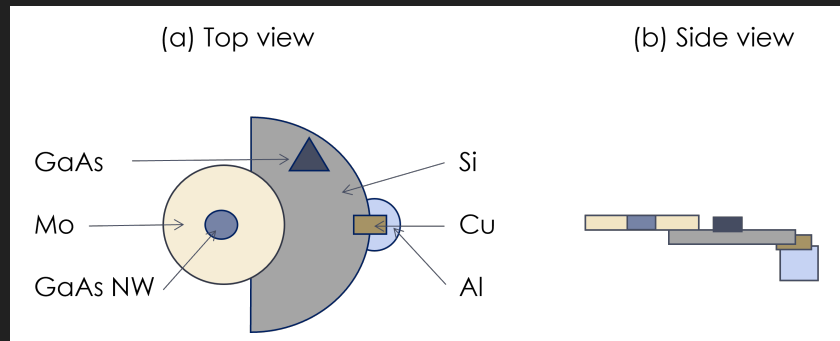


**Figure 3.1:** The sample used for the EDS data collection in the SEM Apreo. (a) is top view and (b) is side view. GaAs is a piece of a GaAs wafer. Mo is a Mo disk. GaAs NW is the TEM grid of Mo with C film and GaAs nanowires. Si is the Si wafer. Cu is the Cu tape. Al is the Al FIB stub. Four spectra with different  $V_{acc}$  was collected on the GaAs, Mo, Si, and GaAs NW. One spectrum was taken on the Cu tape and the Al FIB stub.

with 2 minutes time live. Some spectra were stopped early due to high dead time and thus very long sampling. At least one SE picture was taken for each sampling area.

**(Question for Ton: Is this enough to reproduce the data? I think so.)**

### 3.4 Analysis in AZtec

How to get the results from AZtec, what buttons and settings to use. Which results AZtec gives: elements, concentrations, uncertainties, k-factors, etc.

### 3.5 Extracting the data

The help from Mari and from Daniel. What data I took out from AZtec. Why I needed the k-factors from AZtec.

### 3.6 Analysis in HyperSpy

What HyperSpy needs to do the analysis. What functions I used in HyperSpy. The different quantification methods in HyperSpy. The results from HyperSpy: concentration, uncertainties

### 3.7 Data treatment

In this project the data was also analyzed with new code, which is available on the GitHub. The repository "eds-analysis"<sup>1</sup> contains the code developed throughout the semester, and the repository "eds-analysis-final"<sup>2</sup> contains the

<sup>1</sup><https://github.com/brynjarmorka/eds-analysis/>

<sup>2</sup><https://github.com/brynjarmorka/>

final code. (Brynjar: Make the "eds-analysis-final" repository public.) The code is written in Python and uses Jupyter notebooks. NumPy is used for calculations, SciPy for fitting and peak finding, and Plotly for plotting (Question for Ton: do I to reference these packages?).

### 3.7.1 Normalization

Since the total amount of counts in a spectrum differs with  $V_{acc}$ ,  $I_{beam}$ , DT, etc., the spectra had to be normalized to be able to compare them. (Figure with raw counts of e.g. GaAs?) Initially the spectra were normalized to the highest peak in each spectrum,  $Intensity_{relativetomax} = Counts_{raw} / Counts_{max}$ . Later different methods were explored to see which normalization gave the best results. To measure how good a method was, the area under the peaks of Ga and As in the GaAs spectrum was used. (Brynjar: unfinished.)

(Brynjar: The data can look very different, but a simple scaling can change that drastically. The different normalizations didnt change anything in the quantification.)

### 3.7.2 Gaussian fitting and peak finding

First tried just peak fitting. Then spent a lot of time trying to fit the background, as either linear or 6th order polynomial. Then tried to fit the peaks with a Gaussian function. The final, and best (Brynjar: quantify why best?) solution was to fit with curvefit from SciPy, using a function that is a sum of a 6th order polynomial and n Gaussian curves.

### 3.7.3 Calibration

A third repository, "spectroscopy-channel-calibration"<sup>3</sup>, was made specifically for calibration of spectra, which was used in the course "TFY4255 - Materials Physics" at NTNU, October 2022. The calibration is done with a spectrum of known elements, where the user inputs the energy of the peaks. The user further specifies the channel value of two peaks. The energy of the peaks are available through HyperSpy, or can be set manually from e.g. the X-ray booklet. The code makes a Gaussian fit to the two peaks, to find the true peak center. A plot of the spectrum and the fit are shown, and the user can decide if the fit is good enough. The code then calculates the dispersion, and the zero-offset. In the end the code plots the spectrum with the calibration, and the user can decide if the calibration is good enough. The same calibration is implemented in "eds-analysis-final", but without the plots and the user interaction. (Brynjar: Implement the sentence above.)

### 3.7.4 Background subtraction

I subtracted the background from the spectra to see if the quantification would be better. Linear background subtraction. Sixth order polynomial background subtraction. Additional subtraction?

---

<sup>3</sup><https://github.com/brynjarmorka/spectroscopy-channel-calibration>

### 3.7.5 Area under the peaks

I calculated the area under the peaks to see if working on the raw data could help make the quantification better than AZtec and HyperSpy.

## 3.8 Data from Mari?

(Question for Ton: Do I need this? Is it to compare with my results? Or did you mean to use Maris code to get additional results?)

# Chapter 4

## Results

### 4.1 Introduction

The results are presented in this chapter. The sections follow the structure of the sub-problems in Chapter 1.

### 4.2 Initial quantification

The initial quantification was done on GaAs in AZtec and in HyperSpy as out-of-the-box as possible. The results are presented in

### 4.3 Steps in the analysis

The first sub-problem was to find out what is done with the data at the different steps in the analysis. **(Question for Ton: Is this interesting to write about?)**

### 4.4 Calibration

The calibration of the

### 4.5 Peak and background modelling

The third sub-problem was to find out how the peaks and the background are modelled in a way that is easy to understand.

## **4.6 Background models**

The fourth sub-problem was to find out how different background models affect the quantitative analysis done in HyperSpy.

## **4.7 Failure**

The fifth sub-problem was to find out when the analysis fails, both in AZtec and HyperSpy.

## Chapter 5

# Discussion

### 5.1 Introduction

The discussion is presented in this chapter. ...

### 5.2 Calibration

In Figure 2.5 the calibrated peak of Ga  $K\alpha$  is directly on  $K\alpha_1$  and the  $K\alpha_{\text{HyperSpy}}$ , the emission from  $K\alpha_2$  is missing. The energy difference is too small to differentiate the two peaks in EDS, but the peak has no left-shift, implying that the peak is not a mixture of  $K\alpha_1$  and  $K\alpha_2$ . The peak shape is (Brynjar: calculate the shape), which is close to a perfect Gaussian. There are possible theoretical explanations for the lacking emission from  $K\alpha_2$ . One explanation is the quantum mechanical effect called ..., where two close lines appear as one stronger line. This effect is not only present in EDS, but also in .... Another explanation is that Ga  $K\alpha_2$  could also be weaker than  $K\alpha_1$ , but there is no reason for this to be the case. The take away from this is that the empirical view tends to be good enough for EDS analysis.

# Bibliography

- [1] Joseph I. Goldstein, Dale E. Newbury, Joseph R. Michael, Nicholas W.M. Ritchie, John Henry J. Scott, and David C. Joy. *Scanning Electron Microscopy and X-Ray Microanalysis*. Springer New York, New York, NY, 2018.
- [2] J. Michael Hollas. *Modern spectroscopy*. J. Wiley, Chichester ; Hoboken, NJ, 4th ed edition, 2004.
- [3] Manne Siegbahn. Relations between the K and L Series of the High-Frequency Spectra. *Nature*, 96(2416):676–676, February 1916.
- [4] Albert C Thompson, David T Attwood, Malcolm R Howells, Jeffrey B Kortright, Arthur L Robinson, James H Underwood, Kwang-Je Kim, Janos Kirz, Ingolf Lindau, Piero Pianetta, Herman Winick, Gwyn P Williams, and James H Scofield. *X-Ray Data Booklet*. Lawrence Berkeley National Laboratory, University of California, 2nd ed edition, 2004.